CORAL REEFS

Climate change disables coral bleaching protection on the Great Barrier Reef

Tracy D. Ainsworth,[1*†] Scott F. Heron,[2,3*] Juan Carlos Ortiz,[4,5*] Peter J. Mumby,[4,5] Alana Grech,[6] Daisie Ogawa,[1,7] C. Mark Eakin,[2] William Leggat[1,7*]

Coral bleaching events threaten the sustainability of the Great Barrier Reef (GBR). Here we show that bleaching events of the past three decades have been mitigated by induced thermal tolerance of reef-building corals, and this protective mechanism is likely to be lost under near-future climate change scenarios. We show that 75% of past thermal stress events have been characterized by a temperature trajectory that subjects corals to a protective, sub-bleaching stress, before reaching temperatures that cause bleaching. Such conditions confer thermal tolerance, decreasing coral cell mortality and symbiont loss during bleaching by over 50%. We find that near-future increases in local temperature of as little as 0.5°C result in this protective mechanism being lost, which may increase the rate of degradation of the GBR.

In the past three decades, bleaching events have caused reef-wide declines in coral across the Great Barrier Reef (GBR) (*1*). Coral bleaching is a stress response that results in the loss of intracellular symbiotic dinoflagellates (*Symbiodinium*) and/or their photosynthetic pigments; on a broad spatial scale, bleaching results from extended warm periods (*1*). The frequency and intensity of such bleaching events are expected to increase as sea surface temperature (SST) continues to rise under climate change (*2*, *3*). Acclimatization and adaptation to future temperature conditions have been suggested as mechanisms by which corals may withstand increasing SST, reducing the severity of coral bleaching and ameliorating mortality (*4*–*6*). Although the extent of adaptation remains uncertain (*7*), processes of acclimatization have been studied empirically. An important driver of thermal acclimatization in any organism is the variance of temperature to which it is exposed (*8*). Sub-lethal pre-stress events reset physiological and molecular mechanisms that underpin the innate stress response, and provide a means to survive subsequent stress events (*9*). However, the influence of pre-stress events on thermal tolerance is not well understood in marine ecosystems. Here we show that such pre-stress events do occur on the GBR and serve to increase physiological preparation for the intense thermal stress that results in coral bleaching. We provide experimental evidence to show that this mechanism has probably reduced the impact of historical bleaching events, and we predict that such protective pre-stress events could disappear within a few decades.

To quantify the thermal regimes that GBR corals have experienced, we examined 27 years of satellite-based SST records (at a resolution of 0.5°) and found that 372 thermal stress events, capable of causing bleaching, occurred across 115 reef pixels (*10*). We identified three thermal trajectories associated with past bleaching events,

[1]Australian Research Council Centre of Excellence for Coral Reef Studies, James Cook University, Townsville 4810, Australia. [2]Coral Reef Watch, U.S. National Oceanic and Atmospheric Administration (NOAA), College Park, MD 20740, USA. [3]Marine Geophysical Laboratory, College of Science, Technology and Engineering, James Cook University, Townsville 4811, Australia. [4]Marine Spatial Ecology Lab, School of Biological Sciences, University of Queensland, Brisbane 4072, Australia. [5]Australian Research Council Centre of Excellence for Coral Reef Studies, University of Queensland, Brisbane 4072, Australia. [6]Department of Environmental Sciences, Macquarie University, Sydney 2109, Australia. [7]The College of Public Health, Medical and Veterinary Sciences, James Cook University, Townsville 4810, Australia.
*These authors contributed equally to this work. **†Corresponding author. E-mail: tracy.ainsworth@jcu.edu.au**

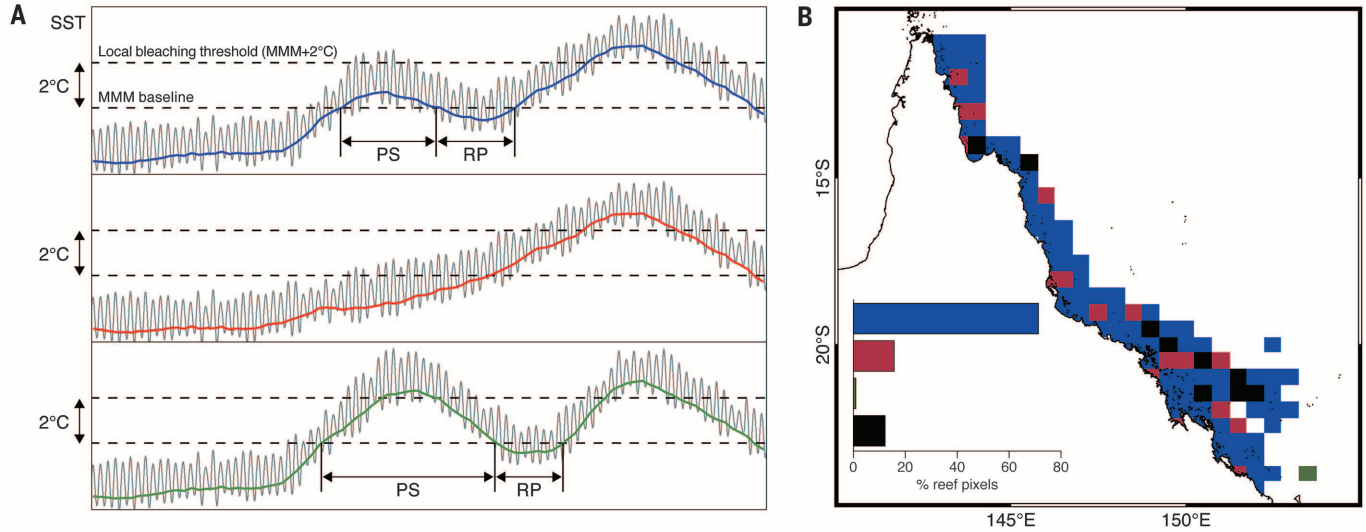

Fig. 1. Sea temperature trajectories before and during coral bleaching stress events on the GBR. (**A**) Schematic of the three temperature trajectories on the GBR during previous (the past 27 years) bleaching level thermal anomalies, where SST reached the local bleaching threshold, 2°C above the local MMM baseline. (Top, blue line) protective trajectory; (middle, red line) single bleaching trajectory; and (bottom, green line) repetitive bleaching trajectory. The black line represents diurnal temperature variation; the colored lines reflect the nighttime-only satellite data. The pre-stress period (PS) is the duration of the pre-stress pulse exceeding the MMM; the recovery period (RP) is the duration below the MMM after the pulse. The horizontal axis spans 90 days. (**B**) The predominant trajectory for each reef pixel ($n = 115$) is shown by color as for (A), except that green shows equal incidence of repetitive and protective trajectories (no pixels were predominated by the repetitive trajectory). Black pixels indicate that the local bleaching threshold (MMM+2°C) was never reached. The histogram (inset) shows the frequency of the predominant trajectories for reef pixels (table S2).

Downloaded from http://science.sciencemag.org/ on January 20, 2017

characterized by the presence and intensity of a pre-stress (sub-bleaching) warming period (Fig. 1A and fig. S1). Warming events were quantified relative to two thresholds: (i) the long-term maximum monthly mean (MMM) temperature, which sets a baseline from which warming can be identified; and (ii) the local coral bleaching threshold (MMM+2°C) (*11*). The predominant trajectory, accounting for 75% of thermal stress events (n = 277), was characterized by an SST event that exceeded the local MMM but remained below the bleaching threshold. The SST then returned below the MMM, for an average recovery period of 10 days, before increasing above the local bleaching threshold (Fig. 1A and table S1); we term this the protective trajectory. The second trajectory was characterized by a direct SST increase from below the MMM to exceed the local bleaching threshold, with no pre-stress or recovery period. This trajectory, which we term the single bleaching trajectory, occurred in 20% (n = 77) of thermal stress events (Fig. 1, A and B). The final trajectory exceeded the local bleaching threshold in two peaks, separated by an average recovery period of 9 days below the local MMM (Fig. 1, A and B, and table S1). We term this the repetitive bleaching trajectory, and it accounted for 5% (n = 18) of identified thermal stress events on the GBR (Fig. 1B).

Having identified three thermal trajectories in situ, we studied the physiological response of corals to each temperature trajectory under experimental conditions, using the model species *Acropora aspera* (*10*). Corals exposed to the protective trajectory underwent characteristic alterations (*12–15*) of the symbiotic organisms' photochemistry and heat stress responses that led to the acquisition of thermal tolerance and reduced bleaching and coral cell death (Fig. 2). Cell death is a conserved response to thermal stress and represents the cellular driver of partial- and whole-colony mortality (*16*). Using a multivariate analysis, we showed that the different temperature trajectories result in distinct expression profiles of stress-related genes during coral bleaching (Fig. 2A and tables S7 and S8). Specifically, the gene expression of corals under the protective trajectory differed significantly from that under both the single bleaching (P = 0.03) and repetitive bleaching (P = 0.02) trajectories, and was more similar to that found in corals not exposed to thermal stress (Fig. 2A). Gene expression in the single bleaching and repetitive bleaching trajectories was indistinguishable (P = 0.422). These gene expression profiles were associated with lower levels of localized cell death under the protective trajectory (30 ± 4% of cells) than either the single bleaching trajectory (56 ± 4%) or repetitive bleaching trajectory (70 ± 2%) (Fig. 2B, C). In addition, the extent of bleaching (*Symbiodinium* loss) was less (P < 0.01) in corals exposed to the protective than either of the other two trajectories (Fig. 2B and table S6). In short, corals and their endosymbiotic *Symbiodinium* acquired thermal tolerance after exposure to the sublethal, pre-stress protective trajectory that has predominated throughout the GBR over the past 27 years. However, corals experiencing the single bleaching and repetitive bleaching trajectories did not acquire thermal tolerance, which resulted in poorer physiological outcomes and a greater loss of symbionts and coral tissue during coral bleaching.

Given that sea temperatures are steadily rising, an obvious concern is that the sub-bleaching temperature event of the protective trajectory could eventually exceed the bleaching threshold, switching events from being protective to becoming increasingly lethal. To examine how climate change is projected to alter our three bleaching trajectories, we applied temperature offsets to the observed 27-year time series of SST (*10*), which implicitly incorporates spatially variable interannual variation and ENSO events (Fig. 3, A to T). We took this approach because climate model predictions are incapable of resolving meaningful spatial variation in the rate of warming across the GBR (*17*). This approach was validated by the correlation between historical annual maximum SST and summer-average SST [linear regression slope = 0.98, coefficient of determination (r^2) = 0.82], which supports the hypothesis that all summer temperatures will increase consistently (fig. S2). Moreover, the drivers of SST pulsing (wind speed, solar radiation, and tidal flow; see the supplementary text) are expected to exhibit less than a 2% change by 2100 under most climate models (*18*). Our simulations project that if SST increases by +2°C, as could occur by 2100 under current warming trajectories, the number of thermal stress events will increase (Fig. 3, A to E). Within these, the proportion of events benefiting from the protective trajectory falls by two-thirds, from 75% (historical) to only 22% (Fig. 3, F to J). Concurrently, the proportion of single bleaching

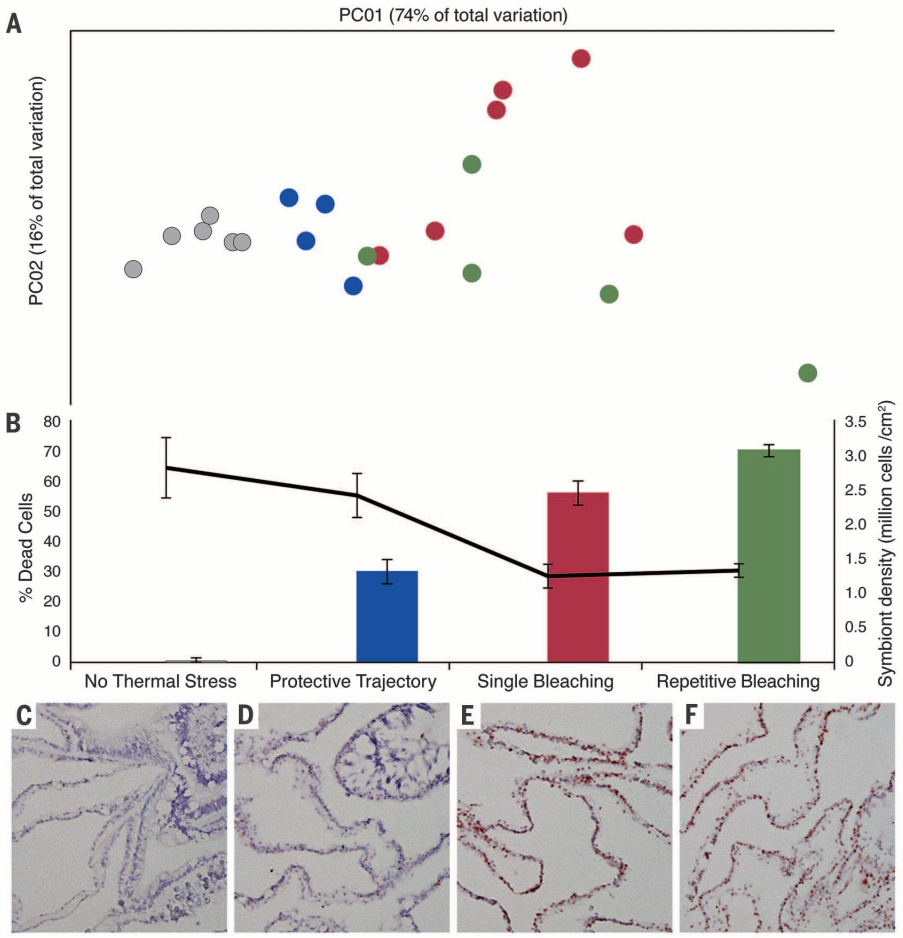

Fig. 2. Effects of temperature trajectories on cell death and *Symbiodinium* cell density of *A. aspera* at bleaching. (**A**) Principal coordinate ordination plot of the gene expression patterns of the apoptotic genes (*Bcl-2*, *Bak*, *Bok*, *Bax*, *Bak*, *Bl*, and *BlR*) under ambient conditions (no thermal stress; white) and the three temperature trajectories: protective (blue), single bleaching (red), and repetitive bleaching (green). Each point represents an individual coral. PC01, principal coordinate ordination axis 1; PC02, principal coordinate ordination axis 2. (**B**) Coral cell death (bars) and *Symbiodinium* density (lines) at bleaching; colors are as for (A). (**C** to **F**) In situ end labeling of coral tissue exposed to (C) ambient conditions and the (D) protective, (E) single bleaching, and (F) repetitive bleaching trajectories. Healthy haematoxylin-counterstained nuclei are stained blue, In situ end-labeled nuclei undergoing cell death are stained red.

Downloaded from http://science.sciencemag.org/ on January 20, 2017

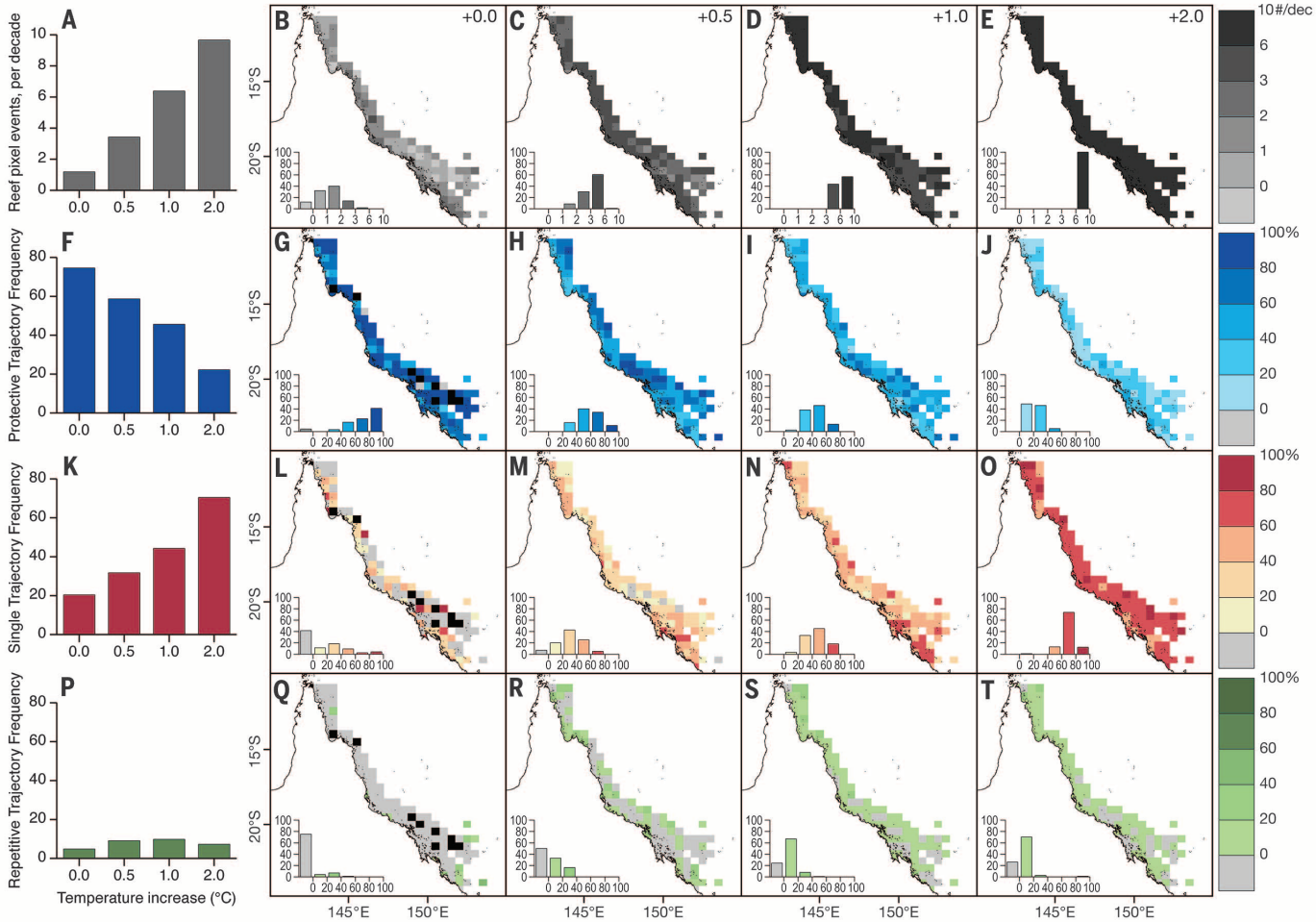

Fig. 3. Projected changes in the frequency of thermal stress events, and SST trajectories, with +0.5°C, +1.0°C, and +2.0°C SST warming. Stress event frequency at 50-km reef pixels (**A**) averaged across the GBR; and spatial distribution under (**B**) recent conditions, and (**C**) +0.5°C, (**D**) +1.0°C, and (**E**) +2.0°C projections. Proportions of events from each trajectory are as follows: (**F** to **J**) protective, (**K** to **O**) single bleaching, (**P** to **T**) repetitive bleaching. Inset histograms show the percentage of reef pixels (vertical axis) with [(B) to (E)] bleaching frequency per decade (horizontal axis) or [(G) to (J), (L) to (O), and (Q) to (T)] trajectory frequency (horizontal axis) for each projected warming. Black pixels in (B), (G), (L), and (Q) indicate that no severe stress events occurred (not present in projected warming).

trajectory events will increase from 21% (Fig. 3, K and L) to 71% (Fig. 3, K and O), implying that thermal stress events become far more lethal for corals. The proportion of repetitive bleaching did not dramatically increase (5 to 7%), but the absolute number increased from 18 to 219 reef pixels experiencing this temperature regime over a 10-year period (Fig. 3, P to T, and table S2).

We predict that most of the reefs that have only experienced the protective trajectory to date (gray in Fig. 3, L and Q) will begin to experience the single and repetitive bleaching trajectories when SST is approximately 0.5°C higher than present (Fig. 3, M and R, and insets in H, M, and R), which will be within 4 decades at historical warming rates (*19*). The sensitivity of reefs to such warming varies geographically (Fig. 3, H, M, and R). For example, reefs in the southern GBR could experience more single bleaching trajectory events at lower temperature increases than elsewhere on the GBR (Fig. 3, L to O). Once there is a 1°C increase in SST, the majority of reefs are likely to experience single trajectory bleaching at least once per decade (Fig. 3, D and N).

The prevalence of an SST trajectory on the GBR that can stimulate thermal tolerance has not previously been recognized, nor has the effect of this induced tolerance on mitigating bleaching events been examined. Acroporid corals, such as *A. aspera* used here, are some of the most important taxa in driving rapid recovery and resilience in Pacific coral reefs (*3*). We therefore integrated our experimental results into a validated simulation model for GBR coral communities (*3*) and evaluated how corals would fare under contrasting emissions scenarios being considered by the Intergovernmental Panel on Climate Change: business-as-usual representative concentration pathway 8.5 (RCP8.5) (*20*) and a low-carbon economy in which CO_2 concentrations are limited to a peak of 450 parts per million by 2040, RCP2.6 (*21*). We used the relative proportions of dead cells within corals that occurred after experimental exposure to the three SST trajectories (Fig. 2B) as a proxy for estimating the extent of coral colony mortality during each type of thermal stress event (*10*). Under business-as-usual (high) carbon emissions, the long-term outlook of reefs was bleak, irrespective of their current thermal trajectory (Fig. 4, A, C, and E); coral cover became low (<5%) toward the end of the century. However, the protective trajectory delayed the onset of this condition by approximately 20 years, which may yet prove to be evolutionarily significant. Moving to aggressive action to reduce greenhouse gas emissions, the outlook for reefs was far better, particularly on reefs experiencing the protective trajectory, where no net long-term decline was predicted (Fig. 4B). However, even under aggressive action, coral cover on reefs exposed to the single and repetitive bleaching trajectories will fall below 5% (Fig. 4, D and F).

Although our ecosystem model now allows for processes of thermal acclimatization, it does not provide for adaptation, mostly because the rates and mechanisms of adaptation in corals remain

Downloaded from http://science.sciencemag.org/ on January 20, 2017

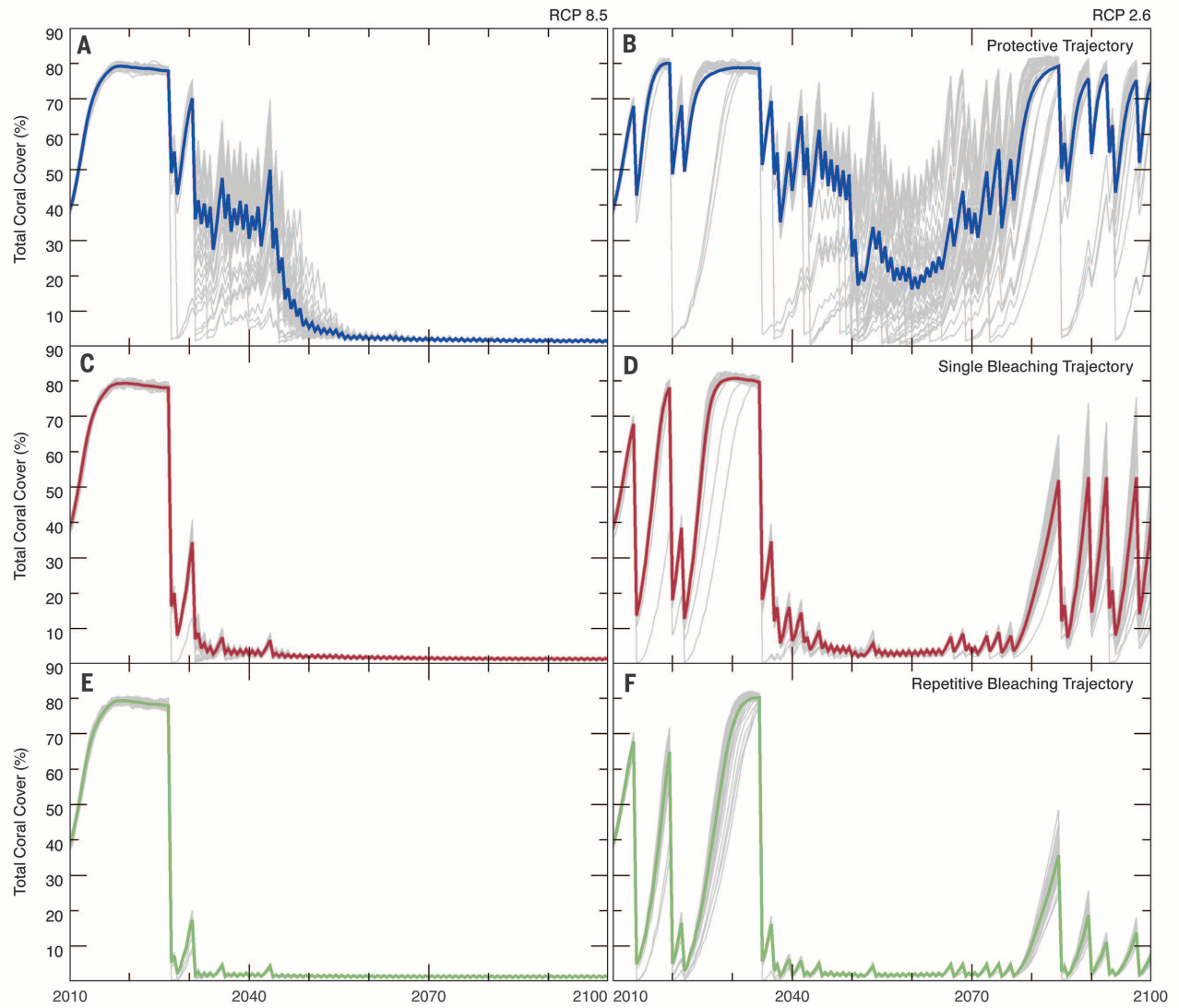

Fig. 4. Coral cover simulations under high (A, C, and E) and low (B, D, and F) CO_2 emission scenarios (RCP8.5 and RCP2.6). This incorporates differential mortality rates associated with protective [(A) and (B)] single bleaching [(C) and (D)] and repetitive bleaching [(E) and (G)] trajectories. Colored lines represent the average coral cover among simulations; gray lines represent the trajectory of each of the 50 simulations for each scenario.

uncertain (*7*). Adaptation may mitigate the impact of climate change and improve the chances of coral reef ecosystem recovery (*4*, *6*, *22*–*24*).

Reefs of the GBR experience a variety of disturbances, only some of which are subject to management interventions. Our analysis reveals that the exposure to sub-lethal pre-stress events varies dramatically among reefs, with some having an inherent level of "protection from" or "preparedness for" the conditions that induce coral bleaching, whereas others experience multiple stress exposures in a single event. Recognizing such spatial variability is important when targeting management actions that aim to mitigate coral reef degradation in the future. For example, local management interventions that reduce cumulative stress impacts (such as impacts caused by pollution, sedimentation, and crown-of-thorns starfish outbreaks) could be prioritized toward reefs that exhibit protective trajectories, thereby serving to minimize biological and physical stressors simultaneously and helping to build ecosystem resilience.

REFERENCES AND NOTES

1. G. De'ath, J. M. Lough, K. E. Fabricius, *Science* **323**, 116–119 (2009).
2. R. van Hooidonk, J. A. Maynard, S. Planes, *Nat. Clim. Change* **3**, 508–511 (2013).
3. J. C. Ortiz, Y.-M. Bozec, N. H. Wolff, C. Doropoulos, P. J. Mumby, *Nat. Clim. Change* **4**, 1090–1094 (2014).
4. J. M. Pandolfi, S. R. Connolly, D. J. Marshall, A. L. Cohen, *Science* **333**, 418–422 (2011).
5. C. R. Voolstra *et al.*, *PLOS One* **6**, e20392 (2011).
6. S. R. Palumbi, D. J. Barshis, N. Traylor-Knowles, R. A. Bay, *Science* **344**, 895–898 (2014).
7. P. J. Mumby, R. van Woesik, *Curr. Biol.* **24**, R413–R423 (2014).
8. J. J. Ruel, M. P. Ayres, *Trends Ecol. Evol.* **14**, 361–366 (1999).
9. D. B. Berry, A. P. Gasch, *Mol. Biol. Cell* **19**, 4580–4587 (2008).
10. Materials and methods are available as supplementary materials on *Science* Online.
11. E. T. Game, M. E. Watts, S. Wooldridge, H. P. Possingham, *Ecol. Appl.* **18**, 670–680 (2008).
12. D. J. Barshis *et al.*, *Proc. Natl. Acad. Sci. U.S.A.* **110**, 1387–1392 (2013).
13. A. J. Bellantuono, C. Granados-Cifuentes, D. J. Miller, O. Hoegh-Guldberg, M. Rodriguez-Lanetty, *PLOS One* **7**, e50685 (2012).
14. T. D. Ainsworth *et al.*, *Sci. Rep.* **1**, 160 (2011).
15. A. J. Bellantuono, O. Hoegh-Guldberg, M. Rodriguez-Lanetty, *Proc. Biol. Sci.* **279**, 1100–1107 (2012).
16. D. Tchernov *et al.*, *Proc. Natl. Acad. Sci. U.S.A.* **108**, 9905–9909 (2011).
17. L. Kwiatkowski, P. J. Halloran, P. Mumby, D. Stephenson, *Clim. Dyn.* **43**, 1483–1496 (2014).
18. D. L. Hartmann *et al.*, *The Physical Science Basis. Contribution of Working Group I to the Fifth Assessment Report of the Intergovernmental Panel on Climate Change* (Cambridge Univ. Press, 2013).
19. J. M. Lough, *J. Environ. Monit.* **10**, 21–29 (2008).
20. K. Riahi *et al.*, *Clim. Change* **109**, 33–57 (2011).
21. D. van Vuuren *et al.*, *Clim. Change* **109**, 95–116 (2011).
22. C. A. Logan, J. P. Dunne, C. M. Eakin, S. D. Donner, *Glob. Change Biol.* **20**, 125–139 (2014).

Downloaded from http://science.sciencemag.org/ on January 20, 2017

23. P. L. Munday, R. R. Warner, K. Monro, J. M. Pandolfi, D. J. Marshall, *Ecol. Lett.* **16**, 1488–1500 (2013).
24. B. M. Riegl, S. J. Purkis, A. S. Al-Cibahy, M. A. Abdel-Moati, O. Hoegh-Guldberg, *PLOS One* **6**, e24802 (2011).

ACKNOWLEDGMENTS

The authors thank the following funding bodies: Australian Research Council Discovery Program grant DP130101421 (awarded to W.L. and T.D.A.); Australian Research Council Super Science Program grant FS110200046 (awarded to Terry P. Hughes, Director, Australian Research Council Centre of Excellence for Coral Reef Studies); Australian Research Council Centre of Excellence for Coral Reef Studies grant CE0561435; the Great Barrier Reef Foundation (Coral Health Grant); the NOAA National Environmental Satellite, Data, and Information Service; and the NOAA Coral Reef Conservation Program. The authors thank N. Wolff for providing SST projections and help in analysis of ecosystem model components and M. De Freitas Prazeres for cell counts. The contents in this manuscript are solely the opinions of the authors and do not constitute a statement of policy, decision, or position on behalf of NOAA or the U.S. government. T.D.A., S.F.H., J.C.O., and W.L. designed the study. T.D.A., D.O., and W.L. conducted experimental procedures and physiological analyses. S.F.H. and C.M.E. conducted SST and oceanographic analyses. J.C.O. and P.J.M. conducted predictive modeling and model validation. T.D.A., S.F.H., J.C.O., P.J.M., A.G., C.M.E., and W.L. wrote and finalized the manuscript. Code for the analysis of SST data is available through contact and collaboration with S. Heron (scott.heron@noaa.gov). Code for the ecosystem model is available through contact and collaboration with J.-C. Ortiz (j.ortiz@uq.edu.au). The NOAA data and code are available from a dedicated web page: http://coralreefwatch.noaa.gov/publications/AinsworthEtAl_2016.php. All data and code are available at FigShare project number 12040: Ecosystems model code and scripts (DOI 10.6084/m9.figshare.3081127); Bleaching on the GBR data release (DOI 10.6084/m9.figshare.3081127); Physiology and gene expression data (DOI 10.6084/m9.figshare.3081064). D.O. is currently employed by Boehringer Ingelheim, Fremont, CA. The authors declare no competing financial interests.

SUPPLEMENTARY MATERIALS

www.sciencemag.org/content/352/6283/338/suppl/DC1
Materials and Methods
Supplementary Text
Figs. S1 to S8
Tables S1 to S8

10 September 2015; accepted 10 March 2016
10.1126/science.aac7125

FOREST ECOLOGY

Belowground carbon trade among tall trees in a temperate forest

Tamir Klein,[1]*† Rolf T. W. Siegwolf,[2] Christian Körner[1]

Forest trees compete for light and soil resources, but photoassimilates, once produced in the foliage, are not considered to be exchanged between individuals. Applying stable carbon isotope labeling at the canopy scale, we show that carbon assimilated by 40-meter-tall spruce is traded over to neighboring beech, larch, and pine via overlapping root spheres. Isotope mixing signals indicate that the interspecific, bidirectional transfer, assisted by common ectomycorrhiza networks, accounted for 40% of the fine root carbon (about 280 kilograms per hectare per year tree-to-tree transfer). Although competition for resources is commonly considered as the dominant tree-to-tree interaction in forests, trees may interact in more complex ways, including substantial carbon exchange.

Stable carbon isotope labeling at the canopy scale is a powerful tool for tracing carbon allocation in forest ecosystems (*1*, *2*). In a dense forest, large quantities of photoassimilates may be exported to mycorrhiza and rhizosphere microbes (*3*–*11*), and hyphae of mycorrhizal fungi can form "underground highways" for carbon and nutrient exchange with and between plants (*9*). It has been suggested that because of the unpredictability of disturbance events and the divergence of responses among plant communities, mycorrhizal fungi and their host plant species are under selective pressure to evolve generality (*9*, *10*). The groups of plants that are interlinked through a common mycorrhizal network are hence termed "guilds" (*10*). The identity and ensemble of fungal species may affect plant community structure and ecosystem productivity (*12*, *13*), with mycorrhiza improving plant fitness by increasing phosphorus and nitrogen uptake (*14*). As a result, mycorrhizal networks are considered an integral part of the autotrophic system (*15*, *16*) and are essential components in ecosystem resilience to change. Yet, these benefits have traditionally been studied from a nutrient supply perspective, and the mycorrhiza "pipeline" was never shown to transfer considerable amounts (>1 g) of mobile carbon compounds among trees (*4*–*10*). In addition to mycorrhizal networks, carbon can be transferred through natural root grafts, which are anatomical fusions between two or more roots. Growth of interconnected trees in situ can be affected directly by the presence of root grafts—for example, by translocation of water and carbohydrates (*17*). Transport across root grafts has been demonstrated in numerous field studies using various methods, from dye injection to the use of radioactive tracers (*18*, *19*), but these grafts are restricted to trees of the same species or, at most, of phylogenetically closely related species (*17*–*20*).

Using a tall canopy crane (*1*, *2*), we continuously labeled five 40-m-tall Norway spruce trees (*Picea abies*) as part of a 5-year free-air CO_2 enrichment experiment (FACE) in a mixed forest in northwest Switzerland (*3*, *21*, *22*) (figs. S1 to S7). Five unlabeled *Picea* trees served as controls (fig. S8). We then measured $\delta^{13}C$ from "tip to toe," including canopy twigs, stems, and fine roots of labeled and unlabeled individuals of *Picea* and of neighboring trees belonging to different taxa (*Fagus sylvatica*, *Pinus sylvestris*, and *Larix decidua*). Except for the five labeled *Picea*, none of the trees were exposed to CO_2 labeling. Using industrial, ^{13}C-depleted CO_2 gas, our canopy labeling made the $\delta^{13}C$ signal of labeled trees more negative by 5.3 per mil (‰) compared to unlabeled control trees: Twig $\delta^{13}C$ was –31.4‰ in labeled and –26.1‰ in unlabeled *Picea* (Fig. 1). New fine roots of labeled *Picea*, isolated from 90 ingrowth cores (figs. S9 and S10) had 2.6‰ lower $\delta^{13}C$ values than the control trees growing in ambient air (no ^{13}C label) (Fig. 1). Almost the same isotopic signal was found among fine roots of similarly tall nonconspecific trees in the neighborhood that were unlabeled and contributed about half of the fine roots recovered from ingrowth cores (Fig. 2A). To validate that fine roots of the other taxa were not confused with those of *Picea*, we excavated roots from *Picea* (control and labeled) and neighboring tree species and traced them to the trunk of origin (figs. S12 to S14). Again, fine roots of these non-*Picea* taxa showed a ^{13}C signal similar to that of their neighboring *Picea* (either control or labeled) but jointly at a 2.6‰ less negative level when ^{13}C-labeled *Picea* was present (Fig. 2B). Hence, both the root-ingrowth-core data (with multiple individuals' input) and the data for intact root systems from three individuals belonging to three different tree genera yielded the same signals. Sapwood $\delta^{13}C$ of the 2010 to 2014 annual rings in stem cores taken at breast height from neighboring and nonneighboring non-*Picea* trees was –27.8 ± 0.1‰ and –26.9 ± 0.1‰, respectively—still a significant difference (P = 0.019).

Because our FACE system operated in the canopy only (20 to 40 m aboveground), tank CO_2, and thus the ^{13}C label, were not present in the understory. This was ascertained first by ^{13}C signals in understory plants, which are exclusively vesicular-arbuscular mycorrhizal: *Paris quadrifolia*, *Mercurialis perennis*, and *Rubus fruticosus*. $\delta^{13}C$ values in rhizomes/root stocks from these three species growing under both unlabeled and labeled *Picea* showed the typical, very negative signals for deep shade plants (from –30.2 to –34.5‰) (fig. S15). Besides differences among species, however, there was absolutely no signal difference between samples collected under unlabeled and labeled *Picea* and no difference between years. Second, we checked the canopy crowns of the trees neighboring the labeled *Picea* individuals for traces

[1]Institute of Botany, University of Basel, Schönbeinstrasse 6, 4056 Basel, Switzerland. [2]Laboratory of Atmospheric Chemistry, Ecosystems Fluxes Research Group, Paul Scherrer Institute, PSI, 5323 Villigen, Switzerland.
***Corresponding author. E-mail: tamir.klein@unibas.ch** †Present address: Institute of Soil, Water, and Environmental Sciences, Agricultural Research Organization Volcani Center, Beit Dagan 50250, Israel.

Downloaded from http://science.sciencemag.org/ on January 20, 2017

EXTENDED PDF FORMAT
SPONSORED BY

www.rndsystems.com

Science
AAAS

Climate change disables coral bleaching protection on the Great Barrier Reef

Tracy D. Ainsworth, Scott F. Heron, Juan Carlos Ortiz, Peter J. Mumby, Alana Grech, Daisie Ogawa, C. Mark Eakin and William Leggat (April 14, 2016)

Science **352** (6283), 338-342. [doi: 10.1126/science.aac7125]

Editor's Summary

Bleaching of the Great Barrier Reef

The Australian Great Barrier Reef (GBR) is one of Earth's most extraordinary natural wonders, but it is vulnerable to climate change. Ainsworth *et al.* have tracked the effects of three decades of increasing heat stress on coral organisms. In the past, pulses of elevated temperatures that presaged hot seasons stimulated the acclimation of coral organisms and resilience to thermal stress. More recently, temperature hikes have been severe and precluded acclimation. The result has been increasing bleaching and death; notably extreme during 2016 in the wake of El Niño.

Science, this issue p. 338

This copy is for your personal, non-commercial use only.

Article Tools Visit the online version of this article to access the personalization and article tools:
http://science.sciencemag.org/content/352/6283/338

Permissions Obtain information about reproducing this article:
http://www.sciencemag.org/about/permissions.dtl

Science (print ISSN 0036-8075; online ISSN 1095-9203) is published weekly, except the last week in December, by the American Association for the Advancement of Science, 1200 New York Avenue NW, Washington, DC 20005. Copyright 2016 by the American Association for the Advancement of Science; all rights reserved. The title *Science* is a registered trademark of AAAS.

Downloaded from http://science.sciencemag.org/ on January 20, 2017